

Periodic striped ground states in Ising models with competing interactions

Alessandro Giuliani¹ and Robert Seiringer²

¹Dipartimento di Matematica Università di Roma Tre
L.go S. L. Murialdo 1, 00146 Roma, Italy

²Institute of Science and Technology Austria,
Am Campus 1, 3400 Klosterneuburg, Austria

Abstract

We consider Ising models in two and three dimensions, with short range ferromagnetic and long range, power-law decaying, antiferromagnetic interactions. We let J be the ratio between the strength of the ferromagnetic to antiferromagnetic interactions. The competition between these two kinds of interactions induces the system to form domains of minus spins in a background of plus spins, or vice versa. If the decay exponent p of the long range interaction is larger than $d+1$, with d the space dimension, this happens for all values of J smaller than a critical value $J_c(p)$, beyond which the ground state is homogeneous. In this paper, we give a characterization of the infinite volume ground states of the system, for $p > 2d$ and J in a left neighborhood of $J_c(p)$. In particular, we prove that the quasi-one-dimensional states consisting of infinite stripes ($d = 2$) or slabs ($d = 3$), all of the same optimal width and orientation, and alternating magnetization, are infinite volume ground states. Our proof is based on localization bounds combined with reflection positivity.

1 Introduction and main results

The problem of proving the emergence of periodic patterns in systems with competing interactions is ubiquitous in several areas of physics, biology and material science [2], ranging from superconductor physics [12], micro-magnetism [10], polymer suspensions [23], martensitic phase transitions [26], quantum Hall systems [14], to metal-oxide-semiconductor field-effect transistors

[37], nuclear matter [31], and many others [5, 6]. In all these systems, experiments or simulations show evidence for the formation of remarkable patterns in suitable regions of the phase diagram. Examples are stripes, bubbles, zig-zag patterns, and columnar phases. The fundamental understanding of these phenomena is still in a primitive stage, mostly based on variational computations and special assumptions on the structure of the low-energy states. There are just a few special cases where the periodicity of the ground state can be proved from first principles [13, 24, 25, 39, 40].

A particularly interesting and poorly understood phenomenon is that of periodic stripe formation [28, 29, 36, 38]. In a series of papers, this phenomenon was studied in Ising and related models with short range attractive and long range repulsive interactions. The method of block reflection positivity led to rigorous proof the existence of periodic striped states both in one dimension [15, 17, 18] and in certain two-dimensional models, including a toy model model for martensitic phase transitions [21] and a model of in-plane spins with discrete orientations and dipolar interactions [16]. However, the physically interesting case of out-of-plane spins with dipolar, or dipolar-like, interactions, which is of great importance for the physics of thin magnetic films, eluded any rigorous treatment so far.

In a recent work [20], we succeeded in computing the specific ground state energy of such a system, with power-law decaying repulsive interactions and decay exponent $p > 2d$ in $d = 2, 3$ space dimensions, asymptotically as the ferromagnetic transition line is approached. Our estimates allowed us to prove emergence of periodic stripe order in a suitable asymptotic sense, but they were not strong enough to fully control the ground state structure, or to prove breaking of rotational symmetry in the ground state. In this paper we extended the ideas of [19, 20] and prove that periodic striped states of optimal width are exact infinite volume ground states. Moreover we give a characterization of infinite volume ground states that are invariant under translations by one (for $d = 2$) or two (for $d = 3$) independent fixed lattice vectors.

The setting is the following: consider Ising models defined by the formal Hamiltonian

$$H(\underline{\sigma}) = -J \sum_{\langle \mathbf{x}, \mathbf{y} \rangle} (\sigma_{\mathbf{x}} \sigma_{\mathbf{y}} - 1) + \sum_{\{\mathbf{x}, \mathbf{y}\}} \frac{(\sigma_{\mathbf{x}} \sigma_{\mathbf{y}} - 1)}{|\mathbf{x} - \mathbf{y}|^p} \quad (1.1)$$

where $\underline{\sigma} \in \{\pm 1\}^{\mathbb{Z}^d}$, $d \geq 2$. The first sum in (1.1) ranges over nearest neighbor pairs in \mathbb{Z}^d , while the second over pairs of distinct sites in \mathbb{Z}^d . For different values of the exponent p , this model is used to describe the effects of frustration induced in magnetic films by the presence of dipolar inter-

actions ($p = 3$) or in charged systems by the presence of an unscreened Coulomb interaction ($p = 1$), as well as many other frustrated systems [1, 3, 4, 5, 6, 7, 8, 9, 11, 22, 27, 28, 30, 32, 33, 34, 35, 38, 41].

In this paper, we choose the exponent p to satisfy the constraint $p > 2d$. As discussed in a previous work [20], if $J > J_c$, with

$$J_c := \sum_{y_1 > 0, \mathbf{y}^\perp \in \mathbb{Z}^{d-1}} \frac{y_1}{(y_1^2 + |\mathbf{y}^\perp|^2)^{p/2}}, \quad (1.2)$$

then there are exactly two ground states, $\sigma_{\mathbf{x}} \equiv +1 \forall \mathbf{x} \in \mathbb{Z}^d$, and $\sigma_{\mathbf{x}} \equiv -1 \forall \mathbf{x} \in \mathbb{Z}^d$. For $J < J_c$, the ground state is *not* uniform, and for J close to J_c it was conjectured to be a periodic striped configuration, i.e., a quasi-one-dimensional periodic configuration of the form $(\underline{\sigma}^{(h)})_{\mathbf{x}} = \text{sign}(\sin(\pi(x_1 + 1/2)/h))$, or translations or rotations thereof, for a suitable stripe width $h \in \mathbb{N}$. In this paper, we prove this conjecture, and characterize the set of infinite volume ground states invariant under translations generated by $d - 1$ lattice vectors.

For simplicity, we restrict the discussion to $d = 2$ and $p > 4$ from now on. Similar considerations are valid in $d = 3$ and $p > 6$ (or, in fact, for any $d \geq 2$ with $p > 2d$). In Appendix A we explain how to adapt the proof to dimension three and higher. Let $e_s(h)$ be the energy per site of $\underline{\sigma}^{(h)}$ computed via (1.1). We let $h^* = \text{argmin}_{h \in \mathbb{N}} e_s(h)$, which is uniquely defined for almost all¹ choices of J . We denote by $\underline{\sigma}^* = \underline{\sigma}^{(h^*)} \in \{\pm 1\}^{\mathbb{Z}^2}$, and we call it an *optimal periodic striped configuration*. Other $4h^* - 1$ optimal periodic striped configurations are obtained from $\underline{\sigma}^*$ via translations and rotations.

In order to state our main result, we also need to introduce the following notions: the configuration $\underline{s} \in \{\pm 1\}^{\mathbb{Z}^2}$ is called an *infinite volume ground state* if it is energetically stable against compactly supported perturbations, that is, for any *finite* $X \subset \mathbb{Z}^2$,

$$H_X(\underline{\sigma}_X | \underline{s}) - H_X(\underline{s}_X | \underline{s}) \geq 0, \quad \forall \underline{\sigma}_X \in \{\pm 1\}^X \quad (1.3)$$

where \underline{s}_X is the restriction of \underline{s} to X , and

$$\begin{aligned} H_X(\underline{\sigma}_X | \underline{s}) &= -J \sum_{\substack{\langle \mathbf{x}, \mathbf{y} \rangle: \\ \mathbf{x}, \mathbf{y} \in X}} (\sigma_{\mathbf{x}} \sigma_{\mathbf{y}} - 1) + \sum_{\substack{\{\mathbf{x}, \mathbf{y}\}: \\ \mathbf{x}, \mathbf{y} \in X}} \frac{(\sigma_{\mathbf{x}} \sigma_{\mathbf{y}} - 1)}{|\mathbf{x} - \mathbf{y}|^p} \\ &\quad - J \sum_{\substack{\mathbf{x} \in X, \mathbf{y} \in X^c: \\ |\mathbf{x} - \mathbf{y}| = 1}} (\sigma_{\mathbf{x}} s_{\mathbf{y}} - 1) + \sum_{\mathbf{x} \in X, \mathbf{y} \in X^c} \frac{(\sigma_{\mathbf{x}} s_{\mathbf{y}} - 1)}{|\mathbf{x} - \mathbf{y}|^p}. \end{aligned} \quad (1.4)$$

¹There are exceptional values of J for which $e_s(h)$ has two minimizers, h^* and $h^* + 1$.

We shall say that two infinite volume ground states are *equivalent*, if they only differ on a finite set. The equivalence class of a given infinite volume ground state is called a *sector*. A sector is *trivial*, if it contains only one element. In terms of these notions, our main result can be summarized as follows.

Theorem 1. *There exists $\varepsilon > 0$ such that, if $J_c - \varepsilon < J < J_c$, then the optimal periodic striped configurations are infinite volume ground states, and their sectors are trivial.*

This result is a corollary of a quantitative lower bound on the energy of spin configurations, which will be formulated in Theorem 3 below, after having introduced a few more definitions. Our quantitative bounds also allow us to characterize the infinite volume ground states that are invariant under translation by a vector $\mathbf{n} \in \mathbb{Z}^2$.

Theorem 2. *Under the same conditions as Theorem 1, any infinite volume ground state \underline{s} that is invariant under translation by a vector $\mathbf{n} = (n_1, n_2) \in \mathbb{Z}^2$ is characterized by the following property: there exists an “interface” of finite width, of the form $\mathcal{I}_{k_1, k_2}(\mathbf{n}) = \{\mathbf{x} \in \mathbb{Z}^2 : \mathbf{x} \cdot \mathbf{n}_\perp \in [k_1, k_2]\}$, where $\mathbf{n}_\perp = (-n_2, n_1)$ and $k_1 < k_2$ are two integers, such that \underline{s} coincides with two of the optimal striped configurations on the two infinite components of $(\mathcal{I}_{k_1, k_2}(\mathbf{n}))^c$.*

Let us now introduce a few more definitions, which are required for the formulation of our quantitative lower bound on the energy of a generic spin configuration.

1.1 On good and bad

1.1.1 Contours and corners

Given $\underline{\sigma} \in \{\pm 1\}^{\mathbb{Z}^2}$, we let $\Delta = \{\mathbf{x} \in \mathbb{Z}^2 : (\underline{\sigma})_{\mathbf{x}} = -1\}$, and $\Gamma(\Delta)$ be its boundary, i.e., the union of bonds of the dual lattice $(\mathbb{Z}^2)^*$ separating a point $\mathbf{x} \in \Delta$ from a point $\mathbf{y} \in \Delta^c$. At every vertex of $\Gamma(\Delta) \cap (\mathbb{Z}^2)^*$, there can be either 2 or 4 sides meeting. In the case of 4 sides, we deform the polygon slightly by “chopping off” the edge from the squares containing a $-$ spin; see Fig. 1.

After the chopping, $\Gamma(\Delta)$ splits into disconnected polygons $\Gamma_1, \Gamma_2, \dots$, which are called *contours*. The points where two orthogonal portions of a contour meet are called *corners*. The sites of the dual lattice where a non-trivial chopping operation took place correspond to two corners. We denote by $N_c(\Gamma_i)$ the number of corners of Γ_i , and $N_c(\Delta) = \sum_i N_c(\Gamma_i)$. Note



Figure 1: In the case that 4 sides of the closed polygon $\Gamma(\Delta)$ meet at a vertex v , we slightly deform $\Gamma(\Delta)$ so that the two squares containing a $-$ spin become disconnected from the vertex itself. Case (a) represents the situation where the minus spins are located at NE and SW of v , before and after the “chopping”. Case (b) represents the situation where the minus spins are located at NW and SE of v , before and after the “chopping”.

that, if $\underline{\sigma}$ is a compactly supported perturbation of $\underline{\sigma}^*$, that is, if the set $\{\mathbf{x} \in \mathbb{Z}^2 : (\underline{\sigma})_{\mathbf{x}} \neq (\underline{\sigma}^*)_{\mathbf{x}}\}$ is finite, then $N_c(\Delta) < +\infty$.

1.1.2 Tiles

Given an integer ℓ , we pave \mathbb{Z}^2 with tiles of side ℓ and, given a tile T , we denote by $\Gamma_T(\Delta)$ the union of the bonds in $\Gamma(\Delta)$ that separate a point in $\Delta \cap T$ from a point in Δ^c . Note that this convention assigns uniquely every bond in $\Gamma(\Delta)$ to one of the tiles. The connected components of $\Gamma_T(\Delta)$ are contained in the contours Γ_1, \dots , and are denoted by $\Gamma_{T,i}$, $i = 1, \dots, r_T$. Given a maximal straight portion of $\Gamma_{T,i}$, we assign to each of its two endpoints a “number of corners”, which can be either $1/2$ or 0 , depending on whether or not the given endpoint coincides with one of the corners in $\cup_{j \geq 1} \Gamma_j$. This assignment induces a notion of “number of corners in the tile T ”, to be denoted by $n_c(T)$, which is the sum of the number of corners of all the endpoints of the straight portions of $\Gamma_{T,i}$, with $i = 1, \dots, r_T$. Note that $n_c(T)$ can be either integer or half-integer, and $\sum_T n_c(T) = N_c(\Delta)$.

1.1.3 Bad tiles and good regions

We now identify the tiles T_i such that either $n_c(T_i) > 0$, or they contain a square of side $\ell/5$ completely contained in Δ or in Δ^c , to be called *hole*. We call these tiles *bad*², and we let \mathcal{N}_B be their number. For later convenience, we also let $\mathcal{N}_B^{\text{hole}}$ be the number of bad tiles containing a hole. The connected components of the complement of $\cup_{i=1}^{\mathcal{N}_B} T_i$, are denoted by G_i , $i = 1, \dots, \mathcal{N}_G$, and are called the *good regions*. By construction, any of these connected

²We shall choose ℓ large compared to the optimal stripe width h^* , which explains why we expect a hole to be energetically unfavorable, hence *bad*.

components contains portions of contours in $\Gamma(\Delta)$ that are all straight with the same orientation, and have no corners. We denote by Γ_{G_i} the union of contours in $\Gamma(\Delta)$ contained in G_i . If the elements of Γ_{G_i} are all vertical, we will say that G_i is *vertically striped*, and *horizontally striped* otherwise. Consider a good region G_i that is vertically (resp. horizontally) striped. We say that R is a “rectangular portion of stripe” in G_i , if R is a rectangle completely contained in Δ or in Δ^c , with its two vertical (resp. horizontal) boundaries both belonging to Γ_{G_i} . We also define the distance between its two vertical (resp. horizontal) boundaries to be the width of R . Finally, we let $A_h(G_i)$ denote the area of the union of all the rectangular portions of stripes of width h in G_i . Note that, if $\underline{\sigma}$ is a compactly supported perturbation of $\underline{\sigma}^*$, then $\sum_{i=1}^{N_G} A_h(G_i)$ is finite, $\forall h \neq h^*$.

We are now in the position of stating our quantitative lower bound on the energy $H_X(\underline{s}_X|\underline{\sigma}^*)$ of a spin configuration \underline{s} with $\underline{\sigma}^*$ boundary conditions.

Theorem 3. *There exist positive constants C_0, C_1, ε such that, if $J_c - \varepsilon < J < J_c$ and $C_0 h^* \leq \ell \leq (C_0(J_c - J))^{-1}$, then for every $\underline{s} \in \{\pm 1\}^{\mathbb{Z}^2}$ and every finite set $X \subset \mathbb{Z}^2$,*

$$\begin{aligned} H_X(\underline{s}_X|\underline{\sigma}^*) &\geq H_X(\underline{\sigma}_X^*|\underline{\sigma}^*) + C_1 \left(N_c + (J_c - J)^{\frac{p-2}{p-3}} \ell^2 \mathcal{N}_B^{\text{hole}} \right) \\ &+ \frac{1}{2} \sum_{h \neq h^*} \sum_{i=1}^{N_G} (e_s(h) - e_s(h^*)) A_h(G_i), \end{aligned} \quad (1.5)$$

where $N_c, \mathcal{N}_B^{\text{hole}}$, and G_i are, respectively, the number of corners, the number of bad tiles containing a hole, and the good regions, associated with the infinite spin configuration $\underline{\sigma} = (\underline{s}_X, \underline{\sigma}_{X^c}^*)$ coinciding with \underline{s}_X on X and with $\underline{\sigma}^*$ on X^c , defined via tiling with squares of side length ℓ as described above.

Remark. Since $h^* \sim (J_c - J)^{-1/(p-3)} \ll (J_c - J)^{-1}$ for small $J_c - J$ (compare with Eq. (2.30) below), the condition on ℓ can be fulfilled for J close to J_c . Note also that $e_s(h^*) \sim (J_c - J)^{(p-2)/(p-3)}$ for small $J_c - J$, which agrees with the factor multiplying $\mathcal{N}_B^{\text{hole}}$ in the second term on the right side of (1.5).

Remark. The prefactor $1/2$ in the second line of (1.5) can be replaced by any number less than 1, at the expense of modifying the constants C_0 and ε .

Theorem 3 implies, in particular, that $\underline{\sigma}^*$ is an infinite volume ground state, and that every state $\underline{\sigma}$ that is a compactly supported perturbation of it, is *not* a ground state, simply because any such state necessarily has

corners and, therefore, by (1.5), it has strictly larger energy than $\underline{\sigma}^*$. This immediately implies Theorem 1.

In order to see that also Theorem 2 is a consequence of Theorem 3, consider an infinite volume ground state \underline{s} that is invariant under translations by an integer vector \mathbf{n} . Let $\Lambda \subset \mathbb{Z}^2$ be a square box of side L , and note that the energy price for changing the boundary conditions from \underline{s} to $\underline{\sigma}^*$ scales like the boundary, that is

$$|H_\Lambda(\underline{\sigma}_\Lambda|\underline{s}) - H_\Lambda(\underline{\sigma}_\Lambda|\underline{\sigma}^*)| \leq 2(J + J_c)|\partial\Lambda| \quad (1.6)$$

for any $\underline{\sigma}_\Lambda$. Using this inequality and the very definition of infinite volume ground state, we have

$$\begin{aligned} H_\Lambda(\underline{\sigma}_\Lambda^*|\underline{\sigma}^*) + 2(J + J_c)|\partial\Lambda| &\geq H_\Lambda(\underline{\sigma}_\Lambda^*|\underline{s}) \geq \\ &\geq H_\Lambda(\underline{s}_\Lambda|\underline{s}) \geq H_\Lambda(\underline{s}_\Lambda|\underline{\sigma}^*) - 2(J + J_c)|\partial\Lambda|. \end{aligned} \quad (1.7)$$

Now we apply Theorem 3, thus obtaining

$$C_1 \left(N_c + (J_c - J)^{\frac{p-2}{p-3}} \ell^2 \mathcal{N}_B^{\text{hole}} \right) + \frac{1}{2} \sum_{h \neq h^*} \sum_{i=1}^{\mathcal{N}_G} (e_s(h) - e_s(h^*)) A_h(G_i) \leq 4(J + J_c)|\partial\Lambda|, \quad (1.8)$$

where $N_c, \mathcal{N}_B^{\text{hole}}$ and G_i refer to the configuration $(\underline{s}_\Lambda, \underline{\sigma}_{\Lambda^c}^*)$. In particular, N_c is bounded by $(\text{const.})L$. Since every corner not at the boundary of Λ is repeated with period \mathbf{n} , there can be at most a finite number of them (modulo translations by \mathbf{n}) independently of L . This means that these corners are all contained in a finite strip $\mathcal{I}_{k_1, k_2}(\mathbf{n})$, as claimed in Theorem 2, with k_1, k_2 independent of L . Similarly, we can argue that the holes and the stripes of width different from h^* are all contained in a finite strip $\mathcal{I}_{k_1, k_2}(\mathbf{n})$. This concludes the proof of Theorem 2, in the case that h^* is unique. As observed above, there are exceptional values of J for which $e_s(h)$ has two minimizers, h^* and $h^* + 1$. In these cases, the discussion above leaves open the possibility that on one of the connected components of $(\mathcal{I}_{k_1, k_2}(\mathbf{n}))^c$ the stripes are not all of the same width. However, this cannot be the case: by proceeding as in [15, Section III.D], one can prove that each pair of neighboring stripes of widths $h^*, h^* + 1$ gives an extra positive contribution to the energy per unit stripe length. Therefore, pairs of stripes of different widths are all contained in a finite strip $\mathcal{I}_{k_1, k_2}(\mathbf{n})$, and Theorem 2 follows.

The rest of the paper is devoted to the proof of Theorem 3.

2 Proof of Theorem 3

The proof of Theorem 3 is divided into several steps, and uses many notations and ideas introduced in [20], which will be recalled here. As a preliminary step, we reduce to plus boundary conditions, which allows us to use the droplet formulation for the energy as in [20], see (2.3) below. Once the energy is expressed in terms of droplets, we can localize the energy in the bad tiles and good regions, by proceeding in a way analogous to [20]. The key technical novelty of this paper, as compared to [20], is an efficient way of estimating the energy in the good regions, which may have a complicated geometrical shape. The crucial estimate is summarized in Lemma 1 below, whose proof is given in Section 2.4.

Before entering the proof, we recall some notation: we let $\tau = 2(J - J_c)$, which is assumed to be negative and small, in absolute value. We recall that h^* is of the order $|\tau|^{-1/(p-3)}$ and the specific energy of an optimal striped configuration, $e_s(h^*)$, is negative and of the order $|\tau|^{(p-2)/(p-3)}$ (compare with (2.30) below).

2.1 Reduction to plus boundary conditions

The $\underline{\sigma}^*$ boundary conditions, while natural in the perspective of proving uniqueness of the ground state, are not particularly convenient for using the droplet representation of [20]. However, a few simple algebraic manipulations allow us to reduce to the same boundary conditions of [20] (that is, plus boundary conditions) in a suitable enlarged box. To see this, rewrite $H_X(\underline{\sigma}_X|\underline{\sigma}^*)$ as

$$H_X(\underline{\sigma}_X|\underline{\sigma}^*) = H_X(\underline{\sigma}_X^*|\underline{\sigma}^*) + \lim_{\Lambda \nearrow \mathbb{Z}^2} [H_\Lambda^{\text{per}}(\underline{\sigma}_X, \underline{\sigma}_{\Lambda \setminus X}^*) - H_\Lambda^{\text{per}}(\underline{\sigma}_\Lambda^*)] \quad (2.1)$$

where Λ is a square box of side L , which we choose to be divisible by $2h^*$, $(\underline{\sigma}_X, \underline{\sigma}_{\Lambda \setminus X}^*)$ is the configuration on Λ whose restriction to $X \subset \Lambda$ (resp. $\Lambda \setminus X$) coincides with $\underline{\sigma}_X$ (resp. $\underline{\sigma}_{\Lambda \setminus X}^*$), and $H_\Lambda^{\text{per}}(\underline{\sigma}_\Lambda) = H_\Lambda(\underline{\sigma}_\Lambda|\underline{\sigma}_\Lambda^{\text{per}})$ is the Hamiltonian with periodic, rather than $\underline{\sigma}^*$, boundary conditions (here $\underline{\sigma}_\Lambda^{\text{per}}$ is the periodic extension of $\underline{\sigma}_\Lambda$ over \mathbb{Z}^2).

Now, $H_\Lambda^{\text{per}}(\underline{\sigma}_\Lambda^*) = e_s(h^*)|\Lambda|$ and $H_\Lambda^{\text{per}}(\underline{\sigma}_X, \underline{\sigma}_{\Lambda \setminus X}^*)$ can be further rewritten in terms of a Hamiltonian with plus boundary conditions:

$$H_\Lambda^{\text{per}}(\underline{\sigma}_X, \underline{\sigma}_{\Lambda \setminus X}^*) = \lim_{M \rightarrow \infty} \frac{1}{M^2} H_{\Lambda_M}^+ ((\underline{\sigma}_X, \underline{\sigma}_{\Lambda \setminus X}^*)^{M^2}) \quad (2.2)$$

where Λ_M is a square box of side LM , to be thought of as the union of M^2 copies of Λ , and $(\underline{\sigma}_X, \underline{\sigma}_{\Lambda \setminus X}^*)^{M^2}$ is a symbol for the configuration on Λ_M

obtained by juxtaposing M^2 copies of $(\underline{\sigma}_X, \underline{\sigma}_{\Lambda \setminus X}^*)$, one in each of the copies of Λ . Moreover, $H_X^+(\underline{\sigma}_X) = H_X(\underline{\sigma}_X | \underline{\sigma}^+)$ indicates the Hamiltonian with plus boundary conditions (here $\underline{\sigma}^+$ is the uniform infinite spin configuration consisting of plus spins everywhere). Finally, for later reference, we introduce the shorthand $\underline{u}_{\Lambda_M}$ for the spin configuration $(\underline{\sigma}_X, \underline{\sigma}_{\Lambda \setminus X}^*)^{M^2}$ on Λ_M , and \underline{u} for the infinite one coinciding with $\underline{u}_{\Lambda_M}$ on Λ_M and with $\underline{\sigma}^+$ on the complement. From now on we shall consider $\underline{u}_{\Lambda_M}$ and \underline{u} fixed once and for all.

2.2 Localization

We now re-express $H_{\Lambda_M}^+(\underline{u}_{\Lambda_M})$ in terms of the droplets representation introduced in [20]. Using the notation introduced in Section 1.1.1, we let Δ be the region of minus spins associated with \underline{u} , $\Gamma(\Delta)$ its boundary, and $\Gamma_1, \dots, \Gamma_r$ the corresponding contours. We also denote by $\mathfrak{G}(\Delta)$ the collection of contours, $\mathfrak{G}(\Delta) = \{\Gamma_1, \dots, \Gamma_r\}$. Note that Δ , $\Gamma(\Delta)$, $\mathfrak{G}(\Delta)$ and r are finite, because of the plus boundary conditions. As in [20], we denote by δ_i the maximal connected components of Δ , and by $\mathcal{D}(\Delta)$ their collection. Given $\delta \in \mathcal{D}(\Delta)$, we also let $\Gamma(\delta)$ be the boundary of δ , and $N_c(\delta)$ its number of corners. In terms of these notations, we can re-express the energy of $\underline{u}_{\Lambda_M}$ as

$$H_{\Lambda_M}^+(\underline{u}_{\Lambda_M}) = 2J \sum_{\Gamma \in \mathfrak{G}(\Delta)} |\Gamma| + \sum_{\delta \in \mathcal{D}(\Delta)} U(\delta) + \frac{1}{2} \sum_{\substack{\delta, \delta' \in \mathcal{D}(\Delta) \\ \delta \neq \delta'}} W(\delta, \delta'), \quad (2.3)$$

where

$$U(\delta) := -2 \sum_{\mathbf{x} \in \delta} \sum_{\mathbf{y} \in \mathbb{Z}^2 \setminus \delta} \frac{1}{|\mathbf{x} - \mathbf{y}|^p}, \quad W(\delta, \delta') := 4 \sum_{\mathbf{x} \in \delta} \sum_{\mathbf{y} \in \delta'} \frac{1}{|\mathbf{x} - \mathbf{y}|^p}. \quad (2.4)$$

Let us consider the partition \mathcal{P} of Λ_M defined by the bad tiles and good regions of Λ_M , in the sense of Section 1.1.3: $\mathcal{P} = \{T_i\}_{i=1}^{\mathcal{N}_B} \cup \{G_i\}_{i=1}^{\mathcal{N}_G}$. We now localize the energy in the elements of \mathcal{P} , by proceeding as in [20, Section 3]. More precisely, we derive a lower bound on the energy $H_{\Lambda_M}^+(\underline{u}_{\Lambda_M})$ in the form of a sum of local energies $E_Q(\mathcal{B}_Q)$, each depending only on the ‘‘bubble configuration’’ \mathcal{B}_Q within the region $Q \in \mathcal{P}$. The notion of bubble configuration was introduced in [20, Section 3] and is recalled here: given $Q \in \mathcal{P}$ and $\delta \in \mathcal{D}$, we denote by $\Gamma_Q(\delta)$ the portion of $\Gamma(\delta)$ belonging to Q . Moreover, if $\delta_Q = \delta \cap Q$, we define $\bar{\delta}_Q^{(1)}, \dots, \bar{\delta}_Q^{(m_Q(\delta))}$ to be the maximal connected components of δ_Q , and $\bar{\Gamma}_Q^{(1)}, \dots, \bar{\Gamma}_Q^{(m_Q(\delta))}$ to be the portions of $\Gamma_Q(\delta)$ belonging to the boundary of $\bar{\delta}_Q^{(1)}, \dots, \bar{\delta}_Q^{(m_Q(\delta))}$, respectively. We shall refer to the pair $(\bar{\delta}_Q^{(i)}, \bar{\Gamma}_Q^{(i)})$ as to a *bubble* in Q originating from δ . We shall indicate

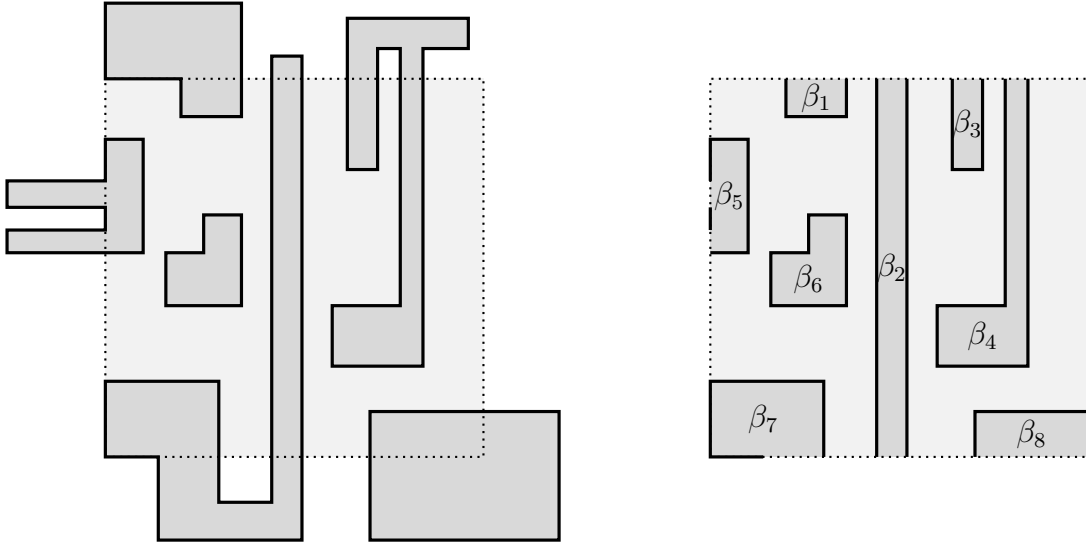


Figure 2: On the left: a square region Q (in light grey, with dotted boundary) and the droplets having non-zero intersection with it. On the right: the corresponding bubble configuration \mathcal{B}_Q after localization in Q . Note that a single droplet can give rise after localization to more than one bubble: e.g., β_2 and β_7 originate from the same droplet, and similarly for β_3 and β_4 . Note also that the contour of a bubble does not necessarily coincide with the boundary of its droplet: in general, it is contained in it, and may even be disconnected (as in the case of β_5 , whose contour consists of two disconnected portions).

by $\mathcal{B}_Q(\delta)$ the set of bubbles in Q originating from δ , and by $\mathcal{B}_Q = \cup_{\delta \in \mathcal{D}} \mathcal{B}_Q(\delta)$ the total set of bubbles in Q . (See Fig. 2.)

Given a bubble $\beta = (\delta_\beta, \Gamma_\beta) \in \mathcal{B}_Q$, we also define its localized self-energy as

$$u_Q(\beta) = - \sum_{b \in \Gamma_\beta} \sum_{\mathbf{n} \neq \mathbf{0}} \frac{\min\{ |n_1|, d_b^Q(\delta_\beta) \}}{|\mathbf{n}|^p}, \quad (2.5)$$

where $d_b^Q(\delta_\beta)$ is the distance between b and the bond $b' \in \Gamma_\beta$ facing it³ in β ,

³ The notion of “bond facing b in β ” is defined as follows. Let us suppose for definiteness that $b \in \Gamma_\beta$ is vertical and that it separates a point $\mathbf{x}_b \in \delta_\beta$ on its immediate right from a point $\mathbf{y}_b = \mathbf{x}_b - (1, 0) \notin \delta_\beta$ on its immediate left. We say that b faces $b' \in \Gamma_\beta$, and vice versa, if: (i) b' is vertical; (ii) b' separates a point $\mathbf{x}_{b'} \in \delta_\beta$ on its immediate left from a point $\mathbf{y}_{b'} = \mathbf{x}_{b'} + (1, 0) \notin \delta_\beta$ on its immediate right; (iii) the points \mathbf{x}_b and $\mathbf{x}_{b'}$ are at the same height, i.e., $[\mathbf{x}_b]_2 = [\mathbf{x}_{b'}]_2$, and all the points on the same row between them belong to δ_β : in other words, $\mathbf{x}_b + (j, 0) \in \delta_\beta$, for all $j = 0, \dots, [\mathbf{x}_{b'}]_1 - [\mathbf{x}_b]_1$. An analogous definition is valid for horizontal bonds. If b does not face any $b' \in \Gamma_\beta$, we say that b faces the boundary of Q .

if there is such a bond, and is infinite, if b faces the boundary of Q . In terms of these notions, our localization bound takes the following form:

$$H_{\Lambda_M}^+(\underline{u}_{\Lambda_M}) \geq \sum_{i=1}^{\mathcal{N}_B} E_{T_i}(\mathcal{B}_{T_i}) + \sum_{i=1}^{\mathcal{N}_G} E_{G_i}(\mathcal{B}_{G_i}), \quad (2.6)$$

where

$$E_{T_i}(\mathcal{B}_{T_i}) = \sum_{\beta \in \mathcal{B}_{T_i}} [2J|\Gamma_\beta| + u_{T_i}(\beta)] + \frac{1}{2} \sum_{\substack{\beta, \beta' \in \mathcal{B}_{T_i}, \\ \beta \neq \beta'}} W(\delta_\beta, \delta_{\beta'}) + 2^{1-p/2} n_c(T_i), \quad (2.7)$$

$$E_{G_i}(\mathcal{B}_{G_i}) = \sum_{\beta \in \mathcal{B}_{G_i}} [2J|\Gamma_\beta| + u_{G_i}(\beta)] + \frac{1}{2} \sum_{\substack{\beta, \beta' \in \mathcal{B}_{G_i}, \\ \beta \neq \beta'}}^* W(\delta_\beta, \delta_{\beta'}), \quad (2.8)$$

and the $*$ on the last sum indicates the following constraint: if the bubbles in G_i are all vertical (resp. horizontal) we only sum over pairs of bubbles that do not overlap after arbitrary translations in the vertical (resp. horizontal) direction.

Proof of (2.6). We start from (2.3). The goal is to bound it from below by a sum of terms, each of which is localized in an element Q of \mathcal{P} . The first term on the right side of (2.3) is already local, i.e., it can be rewritten exactly as $2J \sum_{Q \in \mathcal{P}} \sum_{\beta \in \mathcal{B}_Q} |\Gamma_\beta|$, which leads to the corresponding terms in (2.7) and (2.8). The interaction $W(\delta, \delta')$ on the right side of (2.3) can be rewritten as

$$W(\delta, \delta') = \sum_{Q, Q' \in \mathcal{P}} \sum_{\substack{\beta \in \mathcal{B}_Q(\delta) \\ \beta' \in \mathcal{B}_{Q'}(\delta')}} W(\delta_\beta, \delta_{\beta'}),$$

which is bounded from below by dropping the terms with $Q \neq Q'$ (recall that the interaction is positive), so that

$$\frac{1}{2} \sum_{\substack{\delta, \delta' \in \mathcal{D}(\Delta) \\ \delta \neq \delta'}} W(\delta, \delta') \geq \frac{1}{2} \sum_{Q \in \mathcal{P}} \sum_{\substack{\beta, \beta' \in \mathcal{B}_Q \\ \beta \neq \beta'}}^{**} W(\delta_\beta, \delta_{\beta'}), \quad (2.9)$$

and the $**$ on the sum indicates the constraint that the two droplets δ, δ' in $\mathcal{D}(\Delta)$, which $\delta_\beta, \delta_{\beta'}$ belong to, are different from each other, $\delta \neq \delta'$.

Regarding the second term on the right side of (2.3), we bound it from below by using [20, Eq.(2.9)], that is

$$U(\delta) \geq - \sum_{b \in \Gamma(\delta)} \sum_{\mathbf{n} \neq \mathbf{0}} \frac{\min\{n_1, d_b(\delta)\}}{|\mathbf{n}|^p} + 2^{1-\frac{p}{2}} N_c(\delta) + 4 \sum_{\{\mathbf{x}, \mathbf{y}\} \in \mathcal{P}(\delta)} \frac{1}{|\mathbf{x} - \mathbf{y}|^p}, \quad (2.10)$$

where $d_b(\delta)$ is the distance between b and the bond b' facing it in δ , and $\mathcal{P}(\delta)$ is the set of unordered pairs of distinct sites in δ such that both $\mathcal{C}_{\mathbf{x}\rightarrow\mathbf{y}}^{hv}$ and $\mathcal{C}_{\mathbf{x}\rightarrow\mathbf{y}}^{vh}$ cross at least two bonds of $\Gamma(\delta)$. Here $\mathcal{C}_{\mathbf{x}\rightarrow\mathbf{y}}^{hv}$ is the path on the lattice that goes from \mathbf{x} to \mathbf{y} consisting of two segments, the first horizontal and the second vertical. Similarly, $\mathcal{C}_{\mathbf{x}\rightarrow\mathbf{y}}^{vh}$ is the path on the lattice that goes from \mathbf{x} to \mathbf{y} consisting of two segments, the first vertical and the second horizontal (note that the two paths can coincide, in the case that $x_i = y_i$ for some $i \in \{1, 2\}$).

The first term on the right side of (2.10) can be bounded from below as

$$- \sum_{b \in \Gamma(\delta)} \sum_{\mathbf{n} \neq \mathbf{0}} \frac{\min\{|\mathbf{n}_1|, d_b(\delta)\}}{|\mathbf{n}|^p} \geq \sum_{Q \in \mathcal{D}(\Delta)} \sum_{\beta \in \mathcal{B}_Q(\delta)} u_Q(\beta), \quad (2.11)$$

which, after summation over δ , leads to the terms $\sum_{\beta \in \mathcal{B}_Q} u_Q(\beta)$ in (2.7) and (2.8). The second term on the right side of (2.10) is local and, after summation over δ , can be rewritten as $2^{1-\frac{p}{2}} \sum_{i=1}^{\mathcal{N}_B} n_c(T_i)$ (recall that the good regions have no corners), which leads to the last term on the right side of (2.7). Moreover, the sum over δ of the last term on the right side of (2.10) can be bounded from below by an expression similar to the right side of (2.9), namely

$$\sum_{\delta \in \mathcal{D}(\Delta)} 4 \sum_{\{\mathbf{x}, \mathbf{y}\} \in \mathcal{P}(\delta)} \frac{1}{|\mathbf{x} - \mathbf{y}|^p} \geq \frac{1}{2} \sum_{Q \in \mathcal{P}} \sum_{\substack{\beta, \beta' \in \mathcal{B}_Q \\ \beta \neq \beta'}}^{\dagger} W(\delta_\beta, \delta_{\beta'}), \quad (2.12)$$

where the \dagger on the sum indicates the constraint that $\delta_\beta, \delta_{\beta'}$ belong to the same droplet $\delta \in \mathcal{D}(\Delta)$, and all the pairs of points (\mathbf{x}, \mathbf{y}) in $\delta_\beta \times \delta_{\beta'}$ are such that $\{\mathbf{x}, \mathbf{y}\} \in \mathcal{P}(\delta)$. Combining the right sides of (2.9) and (2.12) we obtain

$$\frac{1}{2} \sum_{Q \in \mathcal{P}} \sum_{\substack{\beta, \beta' \in \mathcal{B}_Q \\ \beta \neq \beta'}}^{\dagger\dagger} W(\delta_\beta, \delta_{\beta'}),$$

where the $\dagger\dagger$ on the sum indicates the constraint that: either $\delta_\beta, \delta_{\beta'}$ belong to different droplets in $\mathcal{D}(\Delta)$, or, if they belong to the same droplet in δ , they are such that all pairs of points (\mathbf{x}, \mathbf{y}) in $\delta_\beta \times \delta_{\beta'}$ are in $\mathcal{P}(\delta)$. Finally, note that: if Q is a bad tile (which is a convex region), then the constraint $\dagger\dagger$ is automatically realized (i.e., it can be dropped), which leads to the second term on the right side of (2.7); if Q is a good region, then the constraint $\dagger\dagger$ is easily seen to be weaker than the one indicated by $*$ in (2.8), which leads to the last term on the right side of (2.8). \square

2.3 Lower bounds on the localized energies

In this subsection we state the key lower bounds on the localized energies in the bad and good regions, and prove that they imply Theorem 3. Recall the definitions of \mathcal{N}_B , $\mathcal{N}_B^{\text{hole}}$ and $A_h(G_i)$ given in Section 1.1.3. Recall also that ℓ is the side length of the tiles, which enters the definition of the partition \mathcal{P} .

Lemma 1. *There exist positive constants c_0 , c_1 and ε such that, if $-\varepsilon < \tau < 0$ and $\ell \geq c_0 h^*$, then the energy E_G of any good region $G \in \mathcal{P}$ satisfies*

$$E_G(\mathcal{B}_G) \geq e_s(h^*)|G| - c_1|\tau||\partial G| + \frac{1}{2} \sum_{h \neq h^*} (e_s(h) - e_s(h^*))A_h(G). \quad (2.13)$$

Lemma 2. *There exist positive constants c_0 , c_2 and ε such that, if $-\varepsilon < \tau < 0$ and $c_0 h^* \leq \ell \leq (c_0|\tau|)^{-1}$, then the energy E_T of any bad tile $T \in \mathcal{P}$ satisfies*

$$E_T(\mathcal{B}_T) \geq \ell^2 e_s(h^*) + c_2 [n_c(T) + |\tau|^{(p-2)/(p-3)} \ell^2 \chi_{\text{hole}}(T)], \quad (2.14)$$

where $\chi_{\text{hole}}(T)$ is equal to 1 if T contains a hole, and 0 otherwise.

Lemma 1 is one of the main technical novelties of this paper, and its proof is described in detail in the next section. The proof of Lemma 2 is simpler, it is an extension of the bounds worked out in [20], and its proof is postponed to Section 2.5.

Combining the two lemmas, we can easily derive Theorem 3. In fact, note that every portion of the boundary ∂G_i of a good region $G_i \in \mathcal{P}$ is adjacent to a bad tile, so that $\sum_{i=1}^{\mathcal{N}_G} |\partial G_i| \leq 4\mathcal{N}_B$. Using this observation, together with the fact that every bad tile either has a positive number of corners (at least 1/2) or a hole, and plugging (2.13) and (2.14) into (2.6), we obtain

$$\begin{aligned} H_{\Lambda_M}^+(\underline{u}_{\Lambda_M}) &\geq e_s(h^*)|\Lambda_M| + \frac{c_2}{2} \left(N_c(\Delta) + |\tau|^{(p-2)/(p-3)} \ell^2 \mathcal{N}_B^{\text{hole}} \right) \\ &\quad + \frac{1}{2} \sum_{h \neq h^*} \sum_{i=1}^{\mathcal{N}_G} (e_s(h) - e_s(h^*))A_h(G_i) \\ &\quad + \mathcal{N}_B \left(\frac{c_2}{2} \min \left\{ \frac{1}{2}, |\tau|^{\frac{p-2}{p-3}} \ell^2 \right\} - 4c_1|\tau|\ell \right). \end{aligned} \quad (2.15)$$

Now, if

$$\frac{8c_1}{c_2} |\tau|^{-1/(p-3)} < \ell < \frac{c_2}{16c_1} |\tau|^{-1},$$

then the expression in parentheses that multiplies \mathcal{N}_B is positive, and we can drop it for the purpose of a lower bound. Via the use of (2.1)–(2.2), we thus arrive at Eq. (1.5).

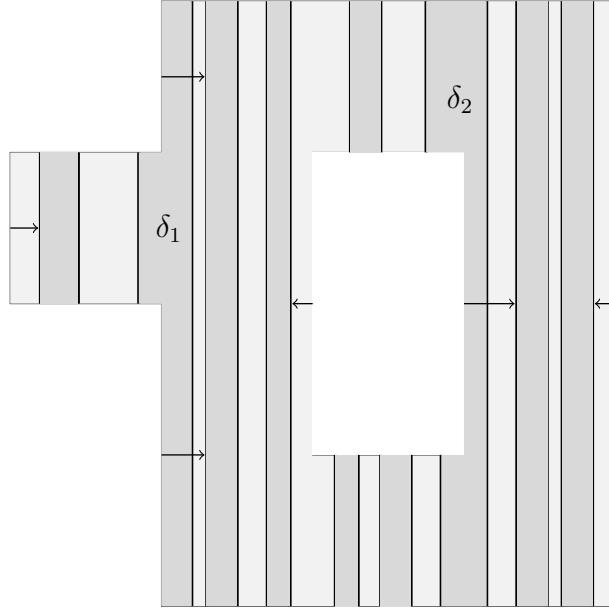


Figure 3: A good region with its bubble configuration. The regions in dark grey are droplets, while those in light grey are their complement. Note that not all of the droplets are rectangular, due to boundary effects. E.g., the droplets δ_1 and δ_2 are not rectangular. The arrows indicate the direction in which the vertical boundary segments move under the deformation described in the text.

2.4 Proof of Lemma 1

2.4.1 Deforming the good regions

We now discuss the proof of Lemma 1. Let us consider a good region $G \in \mathcal{P}$, and let us assume without loss of generality that it only contains vertical stripes. We first want to slightly deform the domain G and correspondingly change the bubble configuration within, in order to make all the bubbles rectangular: here we call “rectangular” a bubble $\beta = (\delta_\beta, \Gamma_\beta)$ such that δ_β is a rectangle and Γ_β is the union of its two vertical sides. Note that, in general, not all the bubbles in G are rectangular, due to boundary effects (in fact, the boundary can partially “cut” a portion of the rectangle, without disconnecting it, see e.g. the droplets δ_1 and δ_2 in Fig. 3).

In order to describe the deformation of G , think of the vertical boundary of G as a union of segments S_i of length ℓ , induced by the tiling described in Sections 1.1.2 and 1.1.3. By construction, every boundary segment S_i faces a portion \tilde{S}_i of length ℓ of the boundary of a *rectangular* bubble in \mathcal{B}_G that is closer than $2\ell/5$ to S_i itself. We now deform the boundary ∂G continuously,

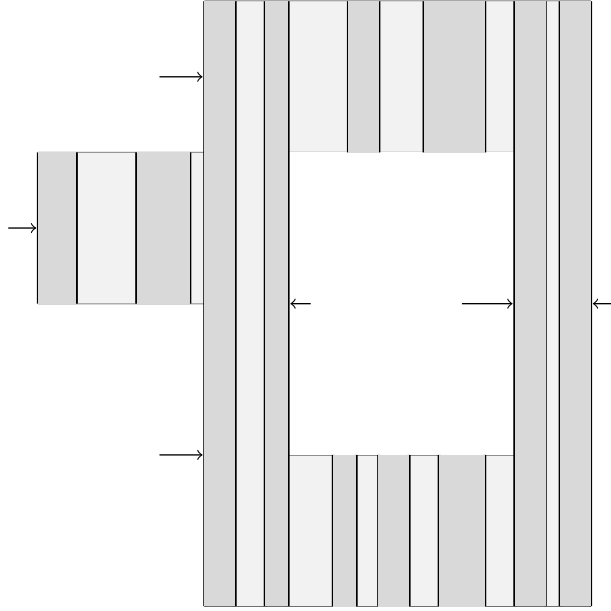


Figure 4: The deformed good region corresponding to the good region of Fig. 3, after the moves of the vertical boundary segments indicated by the arrows. Note that after the deformation all the droplets are rectangular, and all the connected components of the complement of the droplets (the connected light grey regions) are rectangular as well.

by moving the segments S_i towards the interior of G , in such a way that they coincide with \tilde{S}_i ; see Fig. 4.

In this way we increase the boundary of G by at most $|\partial G|$ itself, and we increase the energy by at most $|\tau| \cdot |\partial G|$, which is acceptable for our purposes. We shall denote by G' the new region obtained from G by the deformations we just described, and the new bubble configuration $\mathcal{B}_{G'}$. We have

$$E_G(\mathcal{B}_G) \geq E_{G'}(\mathcal{B}_{G'}) - |\tau| \cdot |\partial G|, \quad (2.16)$$

as just argued.

2.4.2 Slicing and bounding the energy of the good region

The deformed region G' obtained in the previous step is a union of connected horizontal slices g_j of height ℓ , with $j = 1, \dots, N_g$, as shown in Fig. 5. To each slice we associate a sequence of integers $(h_1, w_1, \dots, w_{n-1}, h_n)$, where n is the number of bubbles in $\mathcal{B}_{G'}$ intersecting the slice, h_1, h_2, \dots, h_n are their widths, ordered from left to right, and w_1, w_2, \dots are the spacings between the first and second bubbles, second and third, etc.

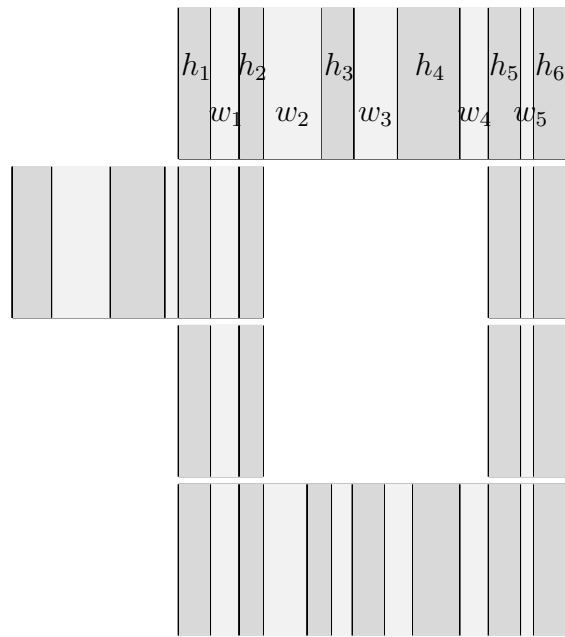


Figure 5: The six slices corresponding to the deformed good region of Fig. 4. For ease of visualization, the slices are drawn slightly detached from each other. As an example, in the first slice we attached the labels h_i and w_i indicating the widths of the stripes (dark grey regions) and of the rectangular regions separating two subsequent stripes from each other (light grey regions).

We also denote by s_i , with $i = 1, \dots, N_s$, the maximal connected segments in the intersection between the horizontal boundary of G' and the boundaries of the droplets in $\mathcal{B}_{G'}$ (note that the boundary of a rectangular bubble does not coincide with its contour: rather, it consists of four segments, two horizontal and two vertical). Note that segments come in pairs: one can say that two segments form a pair if they belong to the boundary of the same droplet. Moreover, to each segment s_j we associate its length $h(s_j)$ and two spacings $w_1(s_j)$, $w_2(s_j)$, which are the horizontal distances from the next droplets (“next” by following the boundary of G') to the left and to the right of s_j . Note that if s_j touches a corner of $\partial G'$, say on its right side, then there may not be any droplet to its right: by following the boundary one may find that the next segment to the right could actually have the same horizontal coordinates, in which case we will assign the value $+\infty$ to $w_2(s_j)$ (and similarly for $w_1(s_j)$ in the case of the next segment on the left); see Fig. 6.

The key ingredient for the proof of Lemma 1 is the following.

Lemma 3. *Given G' and $\mathcal{B}_{G'}$ as above, we have:*

$$E_{G'}(\mathcal{B}_{G'}) \geq \ell \sum_{j=1}^{N_g} e_\infty(h_1^{(j)}, w_1^{(j)}, \dots, h_{n_j}^{(j)}) - \sum_{j=1}^{N_s} f(w_1(s_j), h(s_j), w_2(s_j)), \quad (2.17)$$

where $h_1^{(j)}, w_1^{(j)}, \dots, h_{n_j}^{(j)}$ is the sequence of widths and spacings associated to the slice g_j , and the functions e_∞ and f are defined as follows:

$$\begin{aligned} e_\infty(h_1, w_1, \dots, h_n) &= 4Jn - 2 \sum_{i=1}^n \sum_{\mathbf{x} \in \mathbb{Z}^2 \setminus \{\mathbf{0}\}} \frac{\min\{|x_1|, h_i\}}{|\mathbf{x}|^p} + \\ &\quad + \frac{1}{2} \sum_{\substack{i,j=1,\dots,n \\ i \neq j}} W(l_i, \mathcal{L}(l_j)), \end{aligned} \quad (2.18)$$

where $l_i = \{(x, 0) \in \mathbb{Z}^2 : 0 < x - \sum_{k=1}^{i-1} (h_k + w_k) \leq h_i\}$ and $\mathcal{L}(l_i)$ is the smallest infinite vertical strip containing l_i , that is $\mathcal{L}(l_i) = \{(x, y) \in \mathbb{Z}^2 : 0 < x - \sum_{k=1}^{i-1} (h_k + w_k) \leq h_i, y \in \mathbb{Z}\}$; moreover,

$$f(w_1, h, w_2) = \frac{1}{2} W(\mathcal{L}_h^+, Q_{w_1, h, w_2}) \quad (2.19)$$

where $\mathcal{L}_h^+ = \{(x, y) \in \mathbb{Z}^2 : -h \leq x < 0, y > 0\}$ and $Q_{w_1, h, w_2} = \{(x, y) \in \mathbb{Z}^2 : x < -w_1 - h \text{ or } x \geq w_2, y \leq 0\}$.

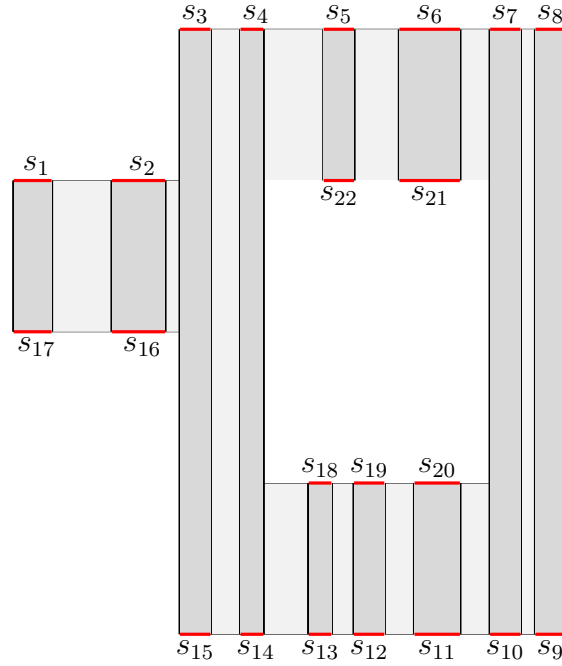


Figure 6: The red segments s_j (color online) for the bubble configuration of Fig. 4 in the deformed good region G' . The segments can be naturally grouped in pairs: two segments form a pair if they belong to the boundary of the same droplet. E.g., s_1 and s_{17} are paired, s_{11} and s_{20} are paired, etc. Every segment s_j comes with its length $h(s_j)$, and with two spacings, the left spacing $w_1(s_j)$ and the right spacing $w_2(s_j)$, corresponding to the distances to the closest droplets to its left and to its right, by moving along the boundary. If one of the endpoints of s_j is a corner of the boundary of G' , then s_j may not have any droplet to its left or right, in which case we let the corresponding spacing to be infinite. In the example in the figure, $w_1(s_1) = w_1(s_{17}) = w_2(s_8) = w_2(s_9) = +\infty$, and all the other spacings are finite.

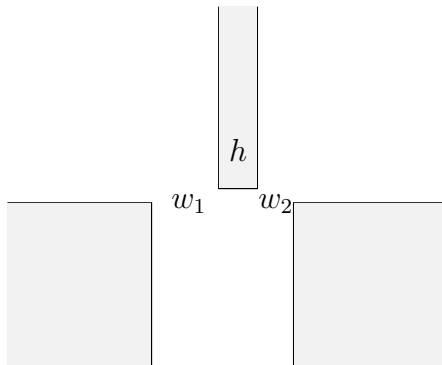


Figure 7: A pictorial representation of the droplets involved in the definitions of $f(w_1, h, w_2)$, which represents the interaction energy of the infinite half strip of width h , with the two quarter spaces to its lower left and lower right. The spacings w_1 and w_2 represent the horizontal distances between the infinite half strip and the quarter space to its left and to its right, respectively.

Remark. e_∞ is the energy per unit vertical length of an infinite vertically striped configuration, and $f(w_1, h, w_2)$ is the interaction energy between the droplets in Fig. 7.

Proof of Lemma 3. First of all, note that the contribution

$$\sum_{\beta \in \mathcal{B}_{G'}} [2J|\Gamma_\beta| + u_{G'}(\beta)]$$

to the energy $E_{G'}(\mathcal{B}_{G'})$ (see (2.8)) is identical to the corresponding contribution in $\ell \sum_{j=1}^{N_g} e_\infty(h_1^{(j)}, w_1^{(j)}, \dots, h_{n_j}^{(j)})$, i.e., to the one arising from the first two terms on the right side of (2.18). Therefore, all we have to prove is that the difference between the interaction terms in $E_{G'}(\mathcal{B}_{G'})$ and in $\ell \sum_{j=1}^{N_g} e_\infty(h_1^{(j)}, w_1^{(j)}, \dots, h_{n_j}^{(j)})$ is bounded from below by the last sum in (2.17).

Let us focus on a given slice g_j and on the intersection of a given bubble β with this slice. The interaction energy of this portion of bubble with all the other bubbles in G' , as it appears in $E_{G'}(\mathcal{B}_{G'})$, is

$$\frac{1}{2} \sum_{\beta' \in \mathcal{B}_{G'}}^* W(\delta_\beta \cap g_j, \delta_{\beta'}), \quad (2.20)$$

where we recall that the $*$ on the sum indicates the constraint that the bubbles β' intersecting β after vertical translations should *not* be included in the sum. Eq. (2.20) can be bounded from below by summing only over the

bubbles β' having non zero intersection with g_j :

$$(2.20) \geq \frac{1}{2} \sum_{\substack{\beta' \in \mathcal{B}_{G'} \\ \beta' \cap g_j \neq \emptyset, \beta' \neq \beta}} W(\delta_\beta \cap g_j, \delta_{\beta'}).$$

The term $\ell \sum_{j=1}^{N_g} e_\infty(h_1^{(j)}, w_1^{(j)}, \dots, h_{n_j}^{(j)})$ on the right side of (2.17) contains a term of that form, with the difference that $\delta_{\beta'}$ is replaced by the infinite vertical strip of the same width containing it. In fact, the interaction term in (2.18) satisfies

$$\ell \sum_{j=1}^{N_g} \sum_{\substack{i, i'=1, \dots, n_j \\ i \neq i'}} W(l_i^{(j)}, \mathcal{L}(l_{i'}^{(j)})) = \sum_{j=1}^{N_g} \sum_{\beta \in \mathcal{B}_{G'}} \sum_{\substack{\beta' \in \mathcal{B}_{G'} \\ \beta' \cap g_j \neq \emptyset, \beta' \neq \beta}} W(\delta_\beta \cap g_j, \mathcal{L}(\delta_{\beta'})), \quad (2.21)$$

where $l_i^{(j)}$ is the analogue of the set l_i defined after (2.18), corresponding to the widths and spacings $h_1^{(j)}, w_1^{(j)}, \dots, h_{n_j}^{(j)}$ associated to the slice g_j . Therefore, what remains to be proved is that

$$\sum_{j=1}^{N_g} \sum_{\beta \in \mathcal{B}_{G'}} \sum_{\substack{\beta' \in \mathcal{B}_{G'} \\ \beta' \cap g_j \neq \emptyset, \beta' \neq \beta}} W(\delta_\beta \cap g_j, \mathcal{L}(\delta_{\beta'} \setminus \delta_{\beta'})) \leq \sum_{j=1}^{N_s} W(\mathcal{L}_{h(s_j)}^+, Q_{w_1(s_j), h(s_j), w_2(s_j)}). \quad (2.22)$$

Let us rewrite the left side of (2.22) as

$$\sum_{\beta' \in \mathcal{B}_{G'}} \sum_{j=1, \dots, N_g} \sum_{\substack{\beta \in \mathcal{B}_{G'} \\ g_j \cap \beta' \neq \emptyset, \beta \neq \beta'}} W(\mathcal{L}(\delta_{\beta'} \setminus \delta_{\beta'}), \delta_\beta \cap g_j). \quad (2.23)$$

Note that the horizontal boundary of $\mathcal{L}(\delta_{\beta'} \setminus \delta_{\beta'})$ consists of two segments s_j, s_k with $h(s_j) = h(s_k)$ and s_j above s_k (these are the pairs of segments mentioned in Section 2.4.2; see Fig. 6), and there is a one-to-one correspondence between summing over β' and summing over these pairs of segments s_j, s_k (which is of course the same as summing over all segments). Moreover, the set $\mathcal{L}(\delta_{\beta'} \setminus \delta_{\beta'})$ is equal to the union of two sets, each of which is a translation, and one also a reflection, of $\mathcal{L}_{h(s_j)}^+$, that is

$$\mathcal{L}(\delta_{\beta'} \setminus \delta_{\beta'}) = \tau_{\beta'}^1 \mathcal{L}_{h(s_j)}^+ \cup \tau_{\beta'}^2 r \mathcal{L}_{h(s_j)}^+ \quad (2.24)$$

for translations $\tau_{\beta'}^1$ and $\tau_{\beta'}^2$, and r denoting reflection about the x_1 -axis.

To conclude, it is enough to note that

$$\bigcup_{i=1, \dots, N_g} \bigcup_{\substack{\beta \in \mathcal{B}_{G'} \\ g_i \cap \beta' \neq \emptyset}} \delta_\beta \cap g_i \subseteq \tau_{\beta'}^1 Q_{w_1(s_j), h(s_j), w_2(s_j)} \cap \tau_{\beta'}^2 Q_{w_1(s_k), h(s_k), w_2(s_k)}, \quad (2.25)$$

which implies the desired inequality (2.22), and thus completes the proof of Lemma 3. \square

2.4.3 Reflection positivity

We now show how to bound from below the right side of (2.17), and how to use the resulting estimate to conclude the proof of Lemma 1. The key step is to use reflection positivity to obtain a lower bound on the e_∞ term. This is an application of the block reflection positivity for one-dimensional spin systems worked out in [15]. The result is the following:

$$e_\infty(h_1, w_1, \dots, h_n) \geq \tau + \sum_{i=1}^n h_i e_s(h_i) + \sum_{i=1}^{n-1} w_i e_s(w_i). \quad (2.26)$$

To see this, note that $e_\infty(h_1, w_1, \dots, h_n) = \lim_{L \rightarrow \infty} H_{\Lambda_L}^{\text{per}}(\underline{\sigma}_{h_1, \dots, h_n})$, where:

1. given a spin configuration $\underline{\sigma}_{\Lambda_L}$ on $\Lambda_L = [1, L] \cap \mathbb{Z}$,

$$H_{\Lambda_L}^{\text{per}}(\underline{\sigma}_{\Lambda_L}) = -J \sum_{i=1}^L (\sigma_i \sigma_{i+1} - 1) + \sum_{1 \leq i < j \leq L} (\sigma_i \sigma_j - 1) v_L(i - j), \quad (2.27)$$

with

$$v_L(x) = \sum_{n, y \in \mathbb{Z}} ((x + nL)^2 + y^2)^{-p/2}, \quad (2.28)$$

and $\sigma_{L+1} \equiv \sigma_1$;

2. the spins in the configuration $\underline{\sigma}_{h_1, \dots, h_n}$ are equal to -1 on the intervals $\{x \in \mathbb{Z} : 0 < x - \sum_{k=1}^{i-1} (h_k + w_k) \leq h_i\}$, and $+1$ otherwise.

Now, $H_{\Lambda_L}^{\text{per}}(\underline{\sigma}_{h_1, \dots, h_n})$ is a one-dimensional spin Hamiltonian with a reflection positive long-range interaction and periodic boundary conditions, of the class considered in [15, 16]. Therefore, we can apply the chessboard estimate proved e.g. in the Appendix of [16]. As a result, using [16, Eqs. (A4)–(A5)] and recalling the fact that the spin configuration $\underline{\sigma}_{h_1, \dots, h_n}$ consists of blocks of alternating sign, of size $h_1, w_1, \dots, h_n, w_n$, with $w_n = w_n(L) = L - (h_1 + w_1 + \dots + h_n)$, we get

$$H_{\Lambda_L}^{\text{per}}(\underline{\sigma}_{\Lambda_L}) \geq \sum_{i=1}^n (h_i e_s(h_i) + w_i e_s(w_i)), \quad (2.29)$$

where $e_s(h)$ is the energy per site (as computed from $H_{\Lambda_L}^{\text{per}}$, in the limit $L \rightarrow \infty$) of the infinite periodic configuration consisting of blocks all of the same size h , and of alternating sign. Note that $e_s(h)$ is the same as the one defined in Section 1 for the two-dimensional model. Finally, to go from (2.29) to (2.26), observe that $\lim_{L \rightarrow \infty} w_n(L) e_s(w_n(L)) = \tau$. This follows, e.g., from the explicit expression of $e_s(h)$, derived in [20, Appendix A]:

$$e_s(h) = \frac{\tau}{h} + \frac{2}{h} \int_0^\infty d\alpha \mu_v(\alpha) \frac{e^{-\alpha}}{(1 - e^{-\alpha})^2} (1 - \tanh \frac{\alpha h}{2}) = \frac{\tau}{h} + \frac{A_p}{h^{p-2}} + O(h^{-p}) \quad (2.30)$$

for large h , where $\mu_v(\alpha)$ is the inverse Laplace transform of the function $v_\infty(x)$ in (2.28), i.e., the function such that $v_\infty(x) = \int_0^\infty d\alpha \mu_v(\alpha) e^{-\alpha x}$, $\forall x > 0$, and A_p is a suitable constant.

Remark. From Eq. (2.30) it follows straight away that the optimal stripe width is $h^* = ((p-2)A_p|\tau|^{-1})^{1/(p-3)}(1 + o(1))$ as $\tau \rightarrow 0$, and also that $e_s(h^*) = \frac{p-3}{p-2} \frac{\tau}{h^*} (1 + o(1))$.

2.4.4 Putting things together

Plugging (2.26) into (2.17) gives

$$\begin{aligned} E_{G'}(\mathcal{B}_{G'}) &\geq |G'| e_s(h^*) + \ell \tau N_g \\ &+ \ell \sum_{j=1}^{N_g} \left[\sum_{k=1}^{n_j} h_k^{(j)} (e_s(h_k^{(j)}) - e_s(h^*)) + \sum_{k=1}^{n_j-1} w_k^{(j)} (e_s(w_k^{(j)}) - e_s(h^*)) \right] \\ &- \sum_{j=1}^{N_s} f(w_1(s_j), h(s_j), w_2(s_j)). \end{aligned} \quad (2.31)$$

Now, $\ell N_g \leq \frac{1}{2} |\partial G'|$ and it remains to show that the sum of the last two lines can be bounded from below by $(\text{const.}) \tau |\partial G'| + \frac{1}{2} \sum_{h \neq h^*} (e_s(h) - e_s(h^*)) A_h(G)$. From the definition of $f(w_1, h, w_2)$ it easily follows that it can be bounded independently of h , as

$$f(w_1, h, w_2) \leq \sum_{i=1,2} \frac{C_2}{w_i^{p-4}} \quad (2.32)$$

for a suitable constant C_2 . Moreover, from (2.30) it follows that

$$e_s(w) - e_s(h^*) \geq \frac{C_3}{w^{p-2}} + \frac{\tau}{w} \quad (2.33)$$

for all $w \geq 1$ and a suitable $C_3 > 0$. Note that the left side is non-negative, while the right side may be negative. A simple consequence of (2.33) is that

$$\frac{C_3}{w^{p-4}} \leq |\tau|w + (C_3|\tau|^{-1})^{\frac{1}{p-3}} w (e_s(w) - e_s(h^*)). \quad (2.34)$$

Using this bound in (2.32) implies that the last line of (2.31) can be bounded as

$$\begin{aligned} & \sum_{j=1}^{N_s} f(w_1(s_j), h(s_j), w_2(s_j)) \leq \\ & \leq \frac{C_2}{C_3} \sum_{j=1}^{N_s} \sum'_{i=1,2} \left[w_i(s_j) |\tau| + (C_3 |\tau|^{-1})^{\frac{1}{p-3}} w_i(s_j) (e_s(w_i(s_j)) - e_s(h^*)) \right], \end{aligned} \quad (2.35)$$

where the prime on the sum indicates the constraint that $w_i(s_j) < \infty$. Now, every spacing $w_i(s_j)$ appears twice in the sum above (because every spacing is to the left or to the right of two different segments $s_j, s_{j'}$), hence $\sum_{j=1}^{N_s} \sum'_{i=1,2} w_i(s_j) \leq 2|\partial G'|$. Similarly,

$$\sum_{j=1}^{N_s} \sum'_{i=1,2} w_i(s_j) (e_s(w_i(s_j)) - e_s(h^*)) \leq 2 \sum_{j=1}^{N_g} \sum_{k=1}^{n_j-1} w_k^{(j)} (e_s(w_k^{(j)}) - e_s(h^*)). \quad (2.36)$$

Therefore, if $\ell \geq 4C_2C_3^{(4-p)/(p-3)} |\tau|^{-1/(p-3)}$,

$$\begin{aligned} E_{G'}(\mathcal{B}_{G'}) & \geq |G'| e_s(h^*) + \tau |\partial G'| \left(\frac{1}{2} + 2 \frac{C_2}{C_3} \right) + \\ & + \ell \sum_{j=1}^{N_g} \left[\sum_{k=1}^{n_j} h_k^{(j)} (e_s(h_k^{(j)}) - e_s(h^*)) + \frac{1}{2} \sum_{k=1}^{n_j-1} w_k^{(j)} (e_s(w_k^{(j)}) - e_s(h^*)) \right]. \end{aligned} \quad (2.37)$$

To complete the proof of Lemma 1, note that $|G'| \leq |G|$, and $|\partial G'| \leq 2|\partial G|$, as already argued above. \square

Remark. The proof of (2.37) is valid for bubble configurations a bit more general than those considered here: in fact, we never used the fact that $\mathcal{B}_{G'}$ has no holes, in the sense explained in Section 1.1.3. The only property we really used is that the bubbles in $\mathcal{B}_{G'}$ are all rectangular with the same orientation.

2.5 Proof of Lemma 2

We proceed similarly to [20, Section 3]. The first step is to estimate the cost of erasing the bubbles with corners. Write $n_c(T) = \sum_{\beta \in \mathcal{B}_T} \nu_c(\beta)$, with $\nu_c(\beta)$

the number of corners associated with the bubble β , which may be an integer or a half-integer. Consider a bubble with $\nu_c(\beta) > 0$. Dropping the positive interaction of this bubble with the others, its contribution to the energy is bounded from below as

$$2J|\Gamma_\beta| + u_T(\beta) + 2^{1-p/2}\nu_c(\beta) \geq \tau|\Gamma_\beta| + 2^{1-\frac{p}{2}}\nu_c(\beta). \quad (2.38)$$

Note that, in order for Γ_β to be very long, the number of corners must be sufficiently large: in formulae (see [20, Eq.(3.10)] and following lines),

$$|\Gamma_\beta| \leq 2\ell + 2\ell\nu_c(\beta). \quad (2.39)$$

If, as we are assuming, $\nu_c(\beta) \geq 1/2$, then $\nu_c(\beta) + 1 \leq 3\nu_c(\beta)$, so that $\nu_c(\beta) \geq |\Gamma_\beta|/(6\ell)$. Inserting this back into (2.38) gives

$$2J|\Gamma_\beta| + u_T(\beta) + 2^{1-p/2}\nu_c(\beta) \geq 2^{-p/2} \frac{|\Gamma_\beta|}{6\ell} \left(1 - 6 \cdot 2^{p/2} |\tau|\ell\right) + 2^{-\frac{p}{2}}\nu_c(\beta). \quad (2.40)$$

The first term on the right side is positive, and, therefore, can be dropped for a lower bound, if $\ell < (6 \cdot 2^{p/2} |\tau|)^{-1}$. Therefore, denoting by \mathcal{S}_T the subset of \mathcal{B}_T consisting of all the bubbles without corners,

$$E_T(\mathcal{B}_T) \geq E_T(\mathcal{S}_T) + 2^{-\frac{p}{2}}n_c(T). \quad (2.41)$$

In order to estimate the energy of the corner-less configuration \mathcal{S}_T we proceed exactly as in the proof Lemma 1. Assume that the contours in \mathcal{S}_T are vertical. We deform the tile T by moving to the right the left vertical boundary of T , until it hits the left vertical contour of a bubble, and vice versa for the right vertical boundary. We call T' and $\mathcal{S}_{T'}$ the new region and configuration obtained after the deformation. In passing from T, \mathcal{S}_T to $T', \mathcal{S}_{T'}$ we increase the energy by at most $2|\tau|\ell$. Now we use the bound (2.37) which, as remarked after (2.37), is valid for all configurations consisting only of rectangular bubbles with the same orientation. The result is

$$\begin{aligned} E_{T'}(\mathcal{S}_{T'}) &\geq e_s(h^*)|T'| + C\tau\ell + \\ &+ \ell \sum_{i=1}^n h_i(e_s(h_i) - e_s(h^*)) + \frac{\ell}{2} \sum_{i=1}^{n-1} w_i(e_s(w_i) - e_s(h^*)), \end{aligned} \quad (2.42)$$

where h_1, \dots, h_n are the widths of the bubbles in $\mathcal{S}_{T'}$, and w_1, \dots, w_{n-1} their separations.

If T contains a hole, then either one of the h_i 's or w_i 's is larger than $\ell/5$, or, the width of T' is smaller than $4\ell/5$. In the first case, one of the terms $\ell h_i(e_s(h_i) - e_s(h^*))$ or $\ell w_i(e_s(w_i) - e_s(h^*))$ is larger than $(\ell^2/5)|e_s(h^*)|$: to see

this recall that $\ell \geq c_0 h^*$, for a large enough constant c_0 , and use (2.30), which implies that $e_s(h)$ is positive for $h \geq \ell/5$ in this case. In the second case, the difference between $e_s(h^*)|T'|$ and $e_s(h^*)|T|$ is larger than $(\ell^2/5)|e_s(h^*)|$. In both cases, we get a gain at least $(\ell^2/5)|e_s(h^*)|$, which is larger than $(\text{const.})\ell^2|\tau|^{(p-2)/(p-3)}$. To conclude the proof, note that under the stated assumptions on ℓ (that is, $c_0 h^* \leq \ell \leq (c_0|\tau|)^{-1}$ for a suitable constant c_0), the error term $(2+C)|\tau|\ell$ is smaller than $c[n_c(T) + |\tau|^{(p-2)/(p-3)}\ell^2\chi_{\text{hole}}(T)]$, where c can be made as small as desired, by increasing c_0 (recall also that by definition of bad tile, either $n_c(T) \geq 1/2$, or $\chi_{\text{hole}}(T) = 1$). This concludes the proof. \square

A The higher-dimensional case

In this appendix we shall detail our main results in the case $d \geq 3$, and explain the main differences in their proof as compared to the two-dimensional case. The starting point is a representation of the energy in terms of droplets as in (2.3), whose boundaries, separating plus spins from minus spins, consist now of $d - 1$ dimensional plaquettes. Tiles are now d -dimensional cubes of side length ℓ , and are used to divide space into good regions and bad cubes, with the good regions only containing “stripes” (i.e., quasi-one-dimensional regions of uniform spins, delimited by two flat parallel interfaces; they are slabs in $d = 3$), which can be oriented in d different directions.

Our first claim concerns the fact that the localization bound (2.6) still holds, with the obvious notion of “corner”, namely $d - 2$ dimensional segments where two plaquettes with different orientation meet. The proof of the analogue of (2.6) in higher dimensions is essentially the same as in $d = 2$, and relies on the analogue of (2.10), whose proof is in [20, App. D].

The key bound in Lemma 1 for the good regions holds verbatim also for general $d \geq 2$. After the modification from G to G' , each stripe has a definite width h but will not be a cuboid, in general; it is bounded by a union of $d - 1$ dimensional cuboids s_k with width h and all other dimensions equal to ℓ . As before, each s_k comes with two numbers, $w_1(s_k)$ and $w_2(s_k)$, measuring the distance to the next slice in the direction perpendicular to the stripes. The analogues of the slices g_j introduced in Sect. 2.4.2 are cylinders with base area ℓ^{d-1} and various heights, which are obtained by adding up the various stripe widths h_i and their separation w_i ; they are oriented perpendicular to the stripes. With these modified definitions, Eq. (2.17) still holds, with ℓ replaced by ℓ^{d-1} in front of the first term on the right side, and $f(w_1, h, w_2)$ now denoting the interaction energy as depicted in Fig. 7, with the upper strip of width h extended by ℓ in the remaining $d - 2$ dimensions, while the

two lower ones are infinite in those directions. This function f satisfies the bound

$$f(w_1, h, w_2) \leq \ell^{d-2} \sum_{i=1,2} \frac{C_2}{w_i^{p-d-2}}. \quad (\text{A.1})$$

As already discussed in [20, App. A], the analogue of (2.30) for general d is

$$e_s(h) = \frac{\tau}{h} + \frac{A_{p,d}}{h^{p-d}} + O(h^{d-p-2}), \quad (\text{A.2})$$

from which it follows that $e_s(h^*) \sim |\tau|^{(p-d)/(p-d-1)}$ and $h^* \sim |\tau|^{-1/(p-d-1)}$ for small τ . Moreover, one easily deduces that (A.1) can be bounded by

$$\frac{C_3}{w^{p-d-2}} \leq |\tau|w + (C_3|\tau|^{-1})^{\frac{1}{p-d-1}} w (e_s(w) - e_s(h^*)), \quad (\text{A.3})$$

which is the analogue of Eq. (2.34). The rest of the proof of Eq. (2.13) for general d remains unchanged.

The analogue of Lemma 2 for general $d \geq 2$ takes the following form:

Lemma 2'. *For given $d \geq 2$, there exist positive constants c_0 , c_2 and ε such that, if $-\varepsilon < \tau < 0$ and $c_0 h^* \leq \ell \leq (c_0 |\tau|)^{-1/(d-1)}$, then the energy E_T of any bad tile $T \in \mathcal{P}$ satisfies*

$$E_T(\mathcal{B}_T) \geq \ell^d e_s(h^*) + c_2 [n_c(T) + |\tau|^{(p-d)/(p-d-1)} \ell^d \chi_{\text{hole}}(T)], \quad (\text{A.4})$$

where $\chi_{\text{hole}}(T)$ is equal to 1 if T contains a hole, and 0 otherwise.

Its proof is a rather straightforward adaptation of the one in $d = 2$, and we refer to [20, App. D], where the necessary changes were described in the case $d = 3$.

Since every portion of the boundary of a good region G_i is adjacent to a bad tile, we have the bound $\sum_{i=1}^{\mathcal{N}_G} |\partial G_i| \leq 2d\ell^{d-1}\mathcal{N}_B$. In combination with the bounds above, this leads to the following generalization of Theorem 3.

Theorem 3'. *For given $d \geq 2$, there exist positive constants C_0 , C_1 , ε such that, if $J_c - \varepsilon < J < J_c$ and $C_0 h^* \leq \ell \leq (C_0 (J_c - J))^{-1/(d-1)}$, then for every $\underline{s} \in \{\pm 1\}^{\mathbb{Z}^d}$ and every finite set $X \subset \mathbb{Z}^d$,*

$$\begin{aligned} H_X(\underline{s}_X | \underline{\sigma}^*) &\geq H_X(\underline{\sigma}_X^* | \underline{\sigma}^*) + C_1 \left(N_c + (J_c - J)^{\frac{p-d}{p-d-1}} \ell^d \mathcal{N}_B^{\text{hole}} \right) \\ &+ \frac{1}{2} \sum_{h \neq h^*} \sum_{i=1}^{\mathcal{N}_G} (e_s(h) - e_s(h^*)) A_h(G_i), \end{aligned} \quad (\text{A.5})$$

where N_c , $\mathcal{N}_B^{\text{hole}}$, and G_i are, respectively, the number of corners, the number of bad tiles containing a hole, and the good regions, associated with the infinite spin configuration $\underline{\sigma} = (\underline{s}_X, \underline{\sigma}_{X^c}^*)$ coinciding with \underline{s}_X on X and with $\underline{\sigma}^*$ on X^c , defined via tiling with squares of side length ℓ as described above.

Theorem 3' implies the analogue of Theorem 1, i.e., the fact that striped configurations with stripe width h^* are infinite volume ground states with trivial sectors for J close to J_c , and also the analogue of Theorem 2, stating that all infinite volume ground states that are invariant under translations by $d - 1$ lattice vectors are characterized by the existence of an interface separating the cubic lattice \mathbb{Z}^d into two components, on each of which the configuration is perfectly striped.

Acknowledgments. The research leading to these results has received funding from the European Research Council under the European Union's Seventh Framework Programme ERC Starting Grant CoMBoS (grant agreement n° 239694), from the Italian PRIN National Grant *Geometric and analytic theory of Hamiltonian systems in finite and infinite dimensions*, and the Austrian Science Fund (FWF), project Nr. P 27533-N27. Part of this work was completed during a stay at the Erwin Schrödinger Institute for Mathematical Physics in Vienna (ESI program 2015 “Quantum many-body systems, random matrices, and disorder”), whose hospitality and financial support is gratefully acknowledged. We also thank Joel Lebowitz and Elliott Lieb for stimulating discussions and their constant encouragement in pursuing this project.

References

- [1] Arlett, J. P. Whitehead, A. B. MacIsaac, and K. De'Bell: *Phase diagram for the striped phase in the two-dimensional dipolar Ising model*, Phys. Rev. B **54**, 3394 (1996).
- [2] P. Ball: *The Self-Made Tapestry: Pattern Formation in Nature*, Oxford University Press, 1999.
- [3] M. Biskup, L. Chayes, and S. A. Kivelson: *On the Absence of Ferromagnetism in Typical 2D Ferromagnets*, Commun. Math. Phys. **274**, 217–231 (2007).
- [4] S. A. Cannas, M. F. Michelon, D. A. Stariolo, F. A. Tamarit: *Ising nematic phase in ultrathin magnetic films: A Monte Carlo study*, Phys. Rev. B **73**, 184425 (2006).
- [5] S. Chakrabarty, V. Dobrosavljevic, A. Seidel, and Z. Nussinov: *Universality of modulation length and time exponents*, Phys. Rev. E **86**, 041132 (2012).

- [6] S. Chakrabarty and Z. Nussinov: *Modulation and correlation lengths in systems with competing interactions*, Phys. Rev. B **84**, 144402 (2011).
- [7] L. Chayes, V. Emery, S. Kivelson, Z. Nussinov, and G. Tarjus: *Avoided critical behavior in a uniformly frustrated system*, Physica A **225**, 129 (1996).
- [8] F. Cinti, O. Portmann, D. Pescia, and A. Vindigni: *One-dimensional Ising ferromagnet frustrated by long-range interactions at finite temperatures*, Phys. Rev. B **79**, 214434 (2009).
- [9] R. Czech and J. Villain: *Instability of two-dimensional Ising ferromagnets with dipole interactions*, J. Phys. Condens. Matter **1**, 619 (1989).
- [10] K. DeBell, A. B. MacIsaac, and J. P. Whitehead: *Dipolar effects in magnetic thin films and quasi-two-dimensional systems*, Rev. Mod. Phys. **72**, 225 (2000).
- [11] E. Edlund and M. Nilsson Jacobi: *Universality of Striped Morphologies*, Phys. Rev. Lett. **105**, 137203 (2010).
- [12] V. J. Emery, S. A. Kivelson, and J. M. Tranquada: *Stripe phases in high-temperature superconductors*, Proc. Nat. Ac. Sc. USA **96**, 8814-8817 (1999).
- [13] L. C. Flatley, F. Theil: *Face-Centered Cubic Crystallization of Atomistic Configurations*, Arch. Rational Mech. Anal. **218**, 363-416 (2015).
- [14] E. Fradkin, S. A. Kivelson: *Liquid-crystal phases of quantum Hall systems*, Phys. Rev. B **59**, 8065 (1999).
- [15] A. Giuliani, J. Lebowitz, E. Lieb: *Ising models with long-range dipolar and short range ferromagnetic interactions*, Phys. Rev. B **74**, 064420 (2006).
- [16] A. Giuliani, J. Lebowitz, E. Lieb: *Striped phases in two-dimensional dipole systems*, Phys. Rev. B **76**, 184426 (2007).
- [17] A. Giuliani, J. Lebowitz, E. Lieb: *Periodic minimizers in 1D local mean field theory*, Commun. Math. Phys. **286**, 163177 (2009).
- [18] A. Giuliani, J. Lebowitz, E. Lieb: *Modulated phases of a 1D sharp interface model in a magnetic field*, Phys. Rev. B **80**, 134420 (2009).

- [19] A. Giuliani, J. Lebowitz, E. Lieb: *Checkerboards, stripes and corner energies in spin models with competing interactions*, Phys. Rev. B **84**, 064205 (2011).
- [20] A. Giuliani, E. H. Lieb and R. Seiringer: *Formation of Stripes and Slabs Near the Ferromagnetic Transition*, Comm. Math. Phys. **331**, 333–350 (2014); and *Realization of stripes and slabs in two and three dimensions*, Phys. Rev. B **88**, 064401 (2013).
- [21] A. Giuliani, S. Müller: *Striped periodic minimizers of a two-dimensional model for martensitic phase transitions*, Commun. Math. Phys. **309**, 313–339 (2012).
- [22] M. Grousson, G. Tarjus, and P. Viot: *Phase diagram of an Ising model with long-range frustrating interactions: A theoretical analysis*, Phys. Rev. E **62**, 7781 (2000).
- [23] C. Harrison et al: *Mechanisms of Ordering in Striped Patterns*, Science **24**, 1558 (2000).
- [24] R. C. Heitmann and C. Radin: *The ground state for sticky disks*, J. Stat. Phys. **22**, 281 (1980).
- [25] T. Kennedy and E. H. Lieb: *An itinerant electron model with crystalline or magnetic long range order*, Physica A **138**, 320 (1986).
- [26] R. V. Kohn and S. Müller: *Branching of twins near an austenite–twinned-martensite interface*, Philos. Mag. A **66**, 697 (1992).
- [27] U. Low, V. J. Emery, K. Fabricius, and S. A. Kivelson: *Study of an Ising model with competing long- and short-range interactions*, Phys. Rev. Lett. **72**, 1918 (1994).
- [28] A. B. MacIsaac, J. P. Whitehead, M. C. Robinson, and K. DeBell: *Striped phases in two-dimensional dipolar ferromagnets*, Phys. Rev. B **51**, 16033 (1995).
- [29] A. Mendoza-Coto, D. A. Stariolo, L. Nicolao: *Nature of long range order in stripe forming systems with long range repulsive interactions*, Phys. Rev. Lett. **114**, 116101 (2015).
- [30] E. Nielsen, R. N. Bhatt, and D. A. Huse: *Modulated phases in magnetic models frustrated by long-range interactions*, Phys. Rev. B **77**, 054432 (2008).

- [31] M. Okamoto, T. Maruyama, K. Yabana, and T. Tatsumi: *Nuclear “pasta” structures in low-density nuclear matter and properties of the neutron-star crust*, Phys. Rev. C **88**, 025801 (2013).
- [32] O. Osenda, F. A. Tamarit, and S. A. Cannas: *Nonequilibrium structures and slow dynamics in a two-dimensional spin system with competing long-range and short-range interactions*, Phys. Rev. E **80**, 021114 (2009).
- [33] S. A. Pighin and S. A. Cannas: *Phase diagram of an Ising model for ultrathin magnetic films: Comparing mean field and Monte Carlo predictions*, Phys. Rev. B **75**, 224433 (2007).
- [34] O. Portmann, A. Golzer, N. Saratz, O. V. Billoni, D. Pescia, and A. Vindigni: *Scaling hypothesis for modulated systems*, Phys. Rev. B **82**, 184409 (2010).
- [35] E. Rastelli, S. Regina, and A. Tassi : *Phase transitions in a square Ising model with exchange and dipole interactions*, Phys. Rev. B **73**, 144418 (2006).
- [36] M. Seul and R. Wolf: *Evolution of disorder in two-dimensional stripe patterns: “Smectic” instabilities and disclination unbinding*, Phys. Rev. Lett. **68**, 2460 (1992).
- [37] B. Spivak and S. A. Kivelson: *Phases intermediate between a two-dimensional electron liquid and Wigner crystal*, Phys. Rev. B **70**, 155114 (2004).
- [38] A. D. Stoycheva and S. J. Singer: *Stripe Melting in a Two-Dimensional System with Competing Interactions*, Phys. Rev. Lett. **84**, 4657 (2000).
- [39] A. Süto: *Crystalline Ground States for Classical Particles*, Phys. Rev. Lett. **95**, 265501 (2005).
- [40] F. Theil: *A Proof of Crystallization in Two Dimensions*, Commun. Math. Phys. **262**, 209 (2006).
- [41] A. Vindigni, N. Saratz, O. Portmann, D. Pescia, and P. Politi: *Stripe width and nonlocal domain walls in the two-dimensional dipolar frustrated Ising ferromagnet*, Phys. Rev. B **77**, 092414 (2008).